

Crystallization and preliminary X-ray diffraction of
Trypanosoma cruzi dUTPaseV. Bernier-Villamor,^{a*} A. Camacho,^a D. González-Pacanoska,^a E. Cedergren-Zeppezauer,^b A. Antson^c and K. S. Wilson^c^aInstituto de Parasitología y Biomedicina 'López Neyra', Ventanilla, 11, PO 18006 Granada, Spain, ^bBiochemistry, Center for Chemistry and Chemical Engineering, Lund University, PO Box 124, S-221 00 Lund, Sweden, and ^cProtein Structure Group, Department of Chemistry, University of York, Heslington, York YO1 5DD, England

Correspondence e-mail: vbernier@ipb.csic.es

Crystals of *Trypanosoma cruzi* dUTPase have been grown. Two different morphologies are observed, depending on the molecular weight of the PEG used as precipitating agent in the mother liquor, both having a hexagonal unit cell with similar dimensions. Complete X-ray diffraction data have been collected to low resolution for one of the forms. The space group is $P6_322$, with unit-cell dimensions $a = 134.15$, $c = 147.05$ Å. Peaks in the self-rotation function and the solvent content are consistent with two molecules of dUTPase per asymmetric unit.

Received 21 May 1998

Accepted 29 July 1998

1. Introduction

dUTPase (deoxyuridine 5'-triphosphate nucleotidohydrolase, E.C. 3.6.1.23) catalyses the hydrolysis of dUTP to dUMP and pyrophosphate. This reaction is important as an intermediate step in the synthesis of thymine nucleotides and has an essential role in maintaining dUTP levels low enough to prevent incorporation of uracil into DNA.

The gene has been demonstrated to be essential in *E. coli* (El-Hajj *et al.*, 1988) and in *Saccharomyces cerevisiae* (Gadsden *et al.*, 1993). Reduced dUTPase activity in mutants of the gene in *E. coli* gives rise to increased incorporation of uracil into DNA (Hochhauser & Weiss, 1978). Enzymes involved in DNA repair eliminate the uracil, but when intracellular levels of dUTP levels are high, extensive incorporation and repair occur leading to DNA fragmentation and cell death (El-Hajj *et al.*, 1992). These toxic effects are also observed with some inhibitors of dihydrofolate reductase and thymidylate synthase used in therapy (Goulian *et al.*, 1980), suggesting a potential use of dUTPase as a new drug target (McIntosh & Haynes, 1997).

dUTPases are present in organisms from viruses to higher eukaryotes. The sequences have an identity ranging from 29 to 36% (McGeoch, 1990), and five amino-acid consensus motifs have been clearly defined. Exceptions are the enzymes from the protozoan parasites *Leishmania major* (Camacho *et al.*, 1997) and *T. cruzi* (Genbank accession number U93211), which show no homology at all with other dUTPases and lack these motifs. Instead they are homologous to one another and in addition share some sequence motifs with an enzyme with a related function,

dCTPase–dUTPase from bacteriophage T4 (Camacho *et al.*, 1997).

The three-dimensional structure has been determined for the enzymes from *E. coli* (Cedergren-Zeppezauer *et al.*, 1992; Larsson *et al.*, 1996), feline immunodeficiency virus (FIV; Prasad *et al.*, 1996), equine infectious anaemia virus (EIAV; Dauter *et al.*, 1999) and human (Mol *et al.*, 1996). They all are trimers with a similar overall structure, each active site being formed with participation of all three subunits in the trimer. However, it is known that there are some monomeric dUTPase structures which have different arrangements of the consensus motifs (Caradonna & Adamkiewicz, 1984; McGeoch, 1990).

Here, we report the crystallization and preliminary X-ray characterization of *T. cruzi* dUTPase, the etiologic agent of Chagas' disease. This dUTPase is a potential target for pharmaceutical inhibitors and the determination of the three-dimensional structure is important for drug design.

2. Experimental procedures

2.1. Enzyme purification

The detailed purification protocol for the enzyme will be reported elsewhere. In brief, the enzyme is overexpressed as a recombinant protein in *E. coli* strain BL21 (DE3) using the pET system (Studier & Moffat, 1986). Purification involves obtaining soluble extract from the cells by sonication in the presence of PMSF, followed by two consecutive chromatographic steps, using hydroxyapatite and DEAE-cellulose as the matrices. The yield is around 20 mg of purified protein per litre of culture. Finally, the buffer is changed by

Sephadex chromatography (Pharmacia GP10 columns) and the enzyme concentrated by ultrafiltration (Centriprep, Amicon) to 20 mg ml⁻¹. Final conditions for the enzyme are 0.1 M imidazole/malate pH 7.2, 5 mM β -mercaptoethanol and 25 mM magnesium chloride.

2.2. Crystallization

Hanging-drop vapour diffusion was used. The droplets, 4 μ l total volume, were made up by mixing 2 μ l of enzyme (20 mg ml⁻¹) with 2 μ l of reservoir solution. The reservoir solution contained 0.1 M Tris-HCl pH 8.3, 30% PEG 1500 (or 25% PEG 3350) and 0.1 M ammonium sulfate. The crystals were grown at room temperature.

X-ray data were collected at cryogenic temperature (120 K) using a MAR Research image plate mounted on a Rigaku RU200 rotating-anode X-ray generator using Cu $K\alpha$ radiation. Crystals were frozen directly from droplet solution if PEG 1500 was used as precipitant. In contrast, the crystals grown in PEG 3350 were soaked in a solution with a higher concentration of PEG

Table 1
Data statistics.

Resolution limits (\AA)	Unique reflections	Completeness (%)	R_{merge}	Reflections with $I < 3\sigma(I)$ (%)
30.00–5.83	2281	96.4	0.068	11.2
5.83–4.84	1635	97.7	0.211	33.2
4.84–4.30	1493	91.3	0.305	43.7
All hkl	5419	95.3	0.061	27.0

(35%) but with the same composition of the other components.

The software used for processing of the data included *DENZO*, *SCALEPACK* (Otwinowski & Minor, 1997) and the *CCP4* suite (Collaborative Computational Project, Number 4, 1994).

3. Results

As a first approach to crystallization two general screens were set up: one according to Jancarik & Kim (1991) (Hampton Screen Kit I) and the so-called 'Footprinting' screen (Stura *et al.*, 1992).

Needle-like crystals were obtained with PEG 4000 as precipitating agent. Conditions were optimized adjusting the pH and the molecular weight of the PEG and using different salts as additives. The addition of salts was essential for the formation of crystals and, from the salts used, ammonium sulfate produced well shaped three-dimensional crystals.

Crystals appeared after two or three days, reaching their maximum size in two weeks. Different morphologies were observed depending on the molecular weight of the PEG. With PEG 3350, the crystals were hexagonal prisms with final dimensions 0.15 \times 0.15 \times 0.2 mm (Fig. 1*a*). PEG 1500 produced crystals in the form of hexagonal bipyramids (Fig. 1*b*). The final dimensions of these crystals are 0.2 \times 0.2 \times 0.25 mm.

X-ray diffraction revealed that both crystal forms have a hexagonal lattice with similar cell dimensions. Complete data were collected for one of the crystals grown in PEG 1500 (Table 1). The space group is $P6_322$, with dimensions $a = 134.15$, $c = 147.05$ \AA . The overall redundancy of reflections is 3.9. Calculation of the self-rotation function suggests that the asymmetric unit contains two mole-

cules, compatible with a solvent content of 60% and a specific volume of 2.98 $\text{\AA}^3 \text{Da}^{-1}$.

4. Discussion

T. cruzi dUTPase has a quite distinct amino-acid sequence from the consensus described for other dUTPases (McGeoch, 1990). The enzyme has a predicted molecular weight of 32065 Da per monomer and an isoelectric point of 5.16. Size-exclusion chromatography determinations suggest that it functions as a dimer (details to be reported elsewhere). dUTPases are described as potential drug targets not yet utilized in therapy (McIntosh & Haynes, 1997). The differences of *T. cruzi* dUTPase make it attractive for structural and functional studies, which will help to design new drugs specific for this enzyme. These drugs could be potentially used in Chagas' disease therapy.

The production of recombinant protein in *E. coli* makes it possible to purify the protein in sufficiently large amounts for crystallization. The purification protocol has been simplified to two chromatographic steps and for crystallization the yield was always sacrificed against purity. Nevertheless, the yield was still high, 20 mg of protein per litre of culture.

The use of different molecular-weight PEGs produced different crystal habits but with similar cell dimensions. The relatively large unit cell and high solvent content may be two reasons why the present crystals do not yet show diffraction to high resolution. Further studies with the present crystals using synchrotron radiation will be performed in order to reach higher resolution.

The data were collected at 120 K. The crystals grown using PEG 1500 as the precipitant did not need a different solution for soaking prior to flash freezing, since the concentration of PEG was high enough to prevent destructive ice formation. For crystals grown in PEG 3350 the cryo solution was made by simply increasing the concentration of the precipitant to 35% (Garman & Schneider, 1997) and maintaining the same concentration of the other components in the mother solution. A short soak in this

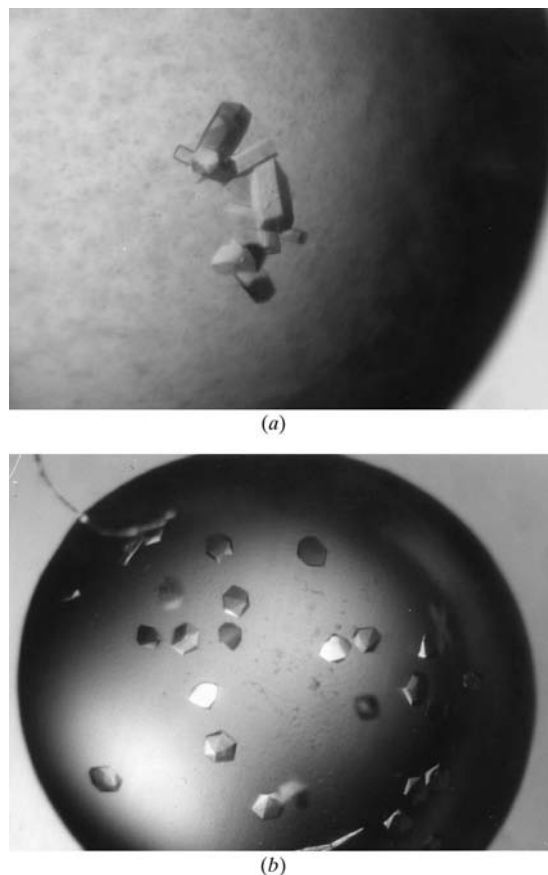


Figure 1
Different crystal morphologies for *Trypanosoma cruzi* dUTPase. (a) Hexagonal prisms (dimensions 0.15 \times 0.15 \times 0.2 mm) using PEG 3350 as the precipitant. (b) Hexagonal bipyramids (dimensions 0.2 \times 0.2 \times 0.25 mm) using PEG 1500.

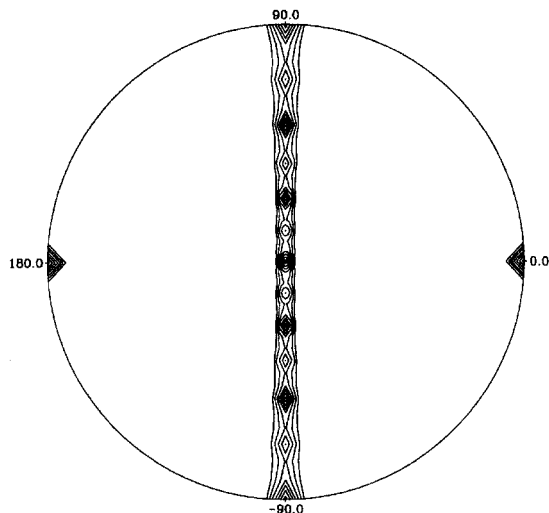


Figure 2
Stereographic projection of self-rotation function with $\kappa = 180$. The φ angle varies from 0° to $\pm 180^\circ$ around the plot, while the ψ angle varies from 0° at the centre to 90° at the outer ring. The crystallographic a axis is vertical (along $\varphi = 90^\circ$, $\psi = 90^\circ$) and the crystallographic c axis is horizontal (along $\varphi = 0^\circ$, $\psi = 90^\circ$). Contouring starts at the 2.0σ level and the interval is 0.25σ .

solution before flash freezing was enough to prevent ice formation.

The size of the unit cell is consistent with two or three molecules per asymmetric unit. To distinguish between these two possibilities, we calculated the self-rotation function $R(\varphi, \psi, \kappa)$ using the program *POLARRFN* from the *CCP4* suite (Collaborative Computational Project, Number 4, 1994). The section $\kappa = 180^\circ$ of the self-rotation function (Fig. 2) shows additional peaks

to those arising from the crystallographic symmetry. Non-crystallographic twofold-symmetry axes could explain these peaks. These axes are perpendicular to the crystallographic sixfold axis; they are midway between the crystallographic twofold axes and at 15° in ψ from them. Hence, there must be a dimer in the asymmetric part of the crystals.

This work is supported by the EC BIOMED project, contract No. BMH4-CT97-2711 (DG12-SSMI). The Instituto de Parasitología y Biomedicina Group in York are also supported by grants from the Spanish Programa Nacional de Biotecnología (BIO97-0659) and the BBSRC, respectively. VB-V is a Predoctoral Fellow of the 'Fundación Ramón Areces' (Spain). We thank Professor Sine Larsen, Center for Crystallographic Studies, University of Copenhagen, for accepting VB-V to attend a course in her laboratory.

References

Camacho, A., Arrebola, R., Peña-Díaz, J., Ruiz-Pérez, L. M. & González-Pacanoska, D. (1997). *Biochem. J.* **325**, 441–447.

Caradonna, S. J. & Adamkiewicz, D. M. (1984). *J. Biol. Chem.* **259**, 5459–5464.
 Cedergren-Zeppezauer, E. S., Larsson, G., Nyman, P. O., Dauter, Z. & Wilson, K. S. (1992). *Nature (London)*, **355**, 740–743.
 Collaborative Computational Project, Number 4 (1994). *Acta Cryst.* **D50**, 760–763.
 Dauter, Z., Persson, R., Rosengren, A. M., Nyman, P. O., Wilson, K. S. & Cedergren-Zeppezauer, E. S. (1999). *J. Mol. Biol.* Submitted.
 El-Hajj, H. H., Wang, L. & Weiss, B. (1992). *J. Bacteriol.* **174**, 4450–4456.
 El-Hajj, H. H., Zhang, H. & Weiss, B. (1988). *J. Bacteriol.* **170**, 1069–1075.
 Gadsden, M. H., McIntosh, E. M., Game, J. C., Wilson, P. J. & Haynes, R. H. (1993). *EMBO J.* **12**, 4425–4431.
 Garman, E. F. & Schneider, T. R. (1997). *J. Appl. Cryst.* **30**, 211–237.
 Goulian, M., Bleile, B. & Tseng, B. Y. (1980). *Proc. Natl Acad. Sci. USA*, **77**, 1956–1960.
 Hochhauser, S. J. & Weiss, B. (1978). *J. Bacteriol.* **134**, 157–166.
 Jancarik, J. & Kim, S.-H. (1991). *J. Appl. Cryst.* **24**, 409–411.
 Larsson, G., Svensson, L. A. & Nyman, P. O. (1996). *Nature Struct. Biol.* **3**, 532–538.
 McGeoch, D. J. (1990). *Nucleic Acids Res.* **18**, 4105–4110.
 McIntosh, E. M. & Haynes, R. H. (1997). *Acta Biochim. Pol.* **44**, 159–171.
 Mol, C. D., Harris, J. M., McIntosh, E. M. & Tainer, J. A. (1996). *Structure*, **4**, 1077–1092.
 Otwinowski, Z. & Minor, W. (1997). *Methods Enzymol.* **276**, 307–326.
 Prasad, G. S., Stura, E. A., McRee, D. E., Laco, G. S., Hasselkus-Light, C., Elder, J. H. & Stout, C. D. (1996). *Protein Sci.* **5**, 2429–2437.
 Studier, F. W. & Moffat, B. A. (1986). *J. Mol. Biol.* **189**, 113–130.
 Stura, E. A., Nemerow, G. R. & Wilson, I. A. (1992). *J. Cryst. Growth*, **122**, 273–285.